Communication

Journal of Photopolymer Science and Technology
Volume 33, Number 2 (2020) 229 – 234 ©2020SPST

Extreme Ultraviolet Photoelectron Spectroscopy on Fluorinated Monolayers: towards Nanolithography on Monolayers

Olivier Lugier[1], Alessandro Troglia[1], Najmeh Sadegh[1], Luc van Kessel[2], Roland Bliem[1,3], Nicola Mahne[4], Stefano Nannarone[4], and Sonia Castellanos[1*]

[1]Advanced Research Center for Nanolithography, Science Park 106, 1098XG Amsterdam, the Netherlands
[2] Delft University of Technology, Department of Imaging Physics, Lorentzweg 1, 2628 CJ Delft, The Netherlands
[3] Institute of Physics, University of Amsterdam, Science Park 904, 1098XH Amsterdam, The Netherlands
[4] CNR-IOM, 34149 Trieste, Italy
**s.castellanos@arcnl.nl*

The semiconductor industry plans to keep fabricating integrated circuits, progressively decreasing there features size, by employing extreme ultraviolet lithography (EUVL). With this method, new designs and concepts for photoresist materials need to be conceived. In this work, we explore an alternative concept to the classic photoresist material by using an organic self-assembled monolayer (SAM) on a gold substrate. The monolayer, composed of a richly fluorinated thiol sensitive to low-energy electrons, is adsorbed on the Au substrate which acts as main EUV-absorber and as the source of photoelectrons and secondary electrons. We investigate the stability of the SAM adsorbed on gold towards EUV radiation by means of in-situ photoelectron spectroscopy. The photoelectron spectra indicate that the monolayer attenuates a significant amount of primary electrons generated in the gold layer. The spectral evolution upon EUV irradiation indicates that the SAM loses a significant amount of its initial fluorine content (ca. 40% at 200 mJ/cm^2). We attribute these chemical changes mostly to the interaction with the electrons generated in the thiol/Au system.

Keywords: EUV Lithography, Self-Assembled Monolayer, Photoelectron spectroscopy

1. Introduction

Future integrated circuits are expected to reach the 10 nm feature size (node) and below in the coming decade. The way chosen by the semiconductor industry to fabricate them in a cost-effective manner is by employing extreme ultraviolet (EUV) lithography. However, the use of such highly energetic EUV photons leads to complex chemical processes, involving the interaction between the photoresist materials and electrons generated upon irradiation [1,2].

In addition, the optical projection will be further improved by using an optical system with higher numerical aperture (NA) in future EUV scanners. Yet, a consequence of using higher NA is having a lower depth of focus (DoF) [3], which requires even thinner films of photoresist material. Therefore, to make an efficient use of this refined technology, new resist concepts should be explored, so that all the targets in the nanopattern resolution and quality can be met.

In this work, we explore an alternative concept to the existing resists. We study a system where a monolayer of organic molecules is adsorbed on the surface of a substrate consisting of a metal with a relatively high EUV photon absorption cross-section. In this way, absorption events occur mainly in the substrate but the chemistry occurs mainly on the organic molecules at the surface. This is because the electrons generated in the substrate upon photon absorption can damage the molecules on top. Turchanin et al. proved that indeed EUV lithography can be performed on self-assembled monolayers (SAMs) adsorbed on gold, though very high doses seemed to be required [4].

Yet, the reactivity of organic molecules towards

Received March 11, 2020
Accepted March 29, 2020

electrons is very much dependent on the molecular structure [5]. Here, we studied a SAM based on a fluorinated carbon chain (Fig. 1). It has been reported in the literature that C-F bonds are prone to cleave with electrons [6,7] and, in particular, fluorinated thiols undergo many chemical reactions when exposed to low-energy electrons [8]. It is foreseen that chemical damage induced in a fluorinated monolayer could provide high chemical contrast between exposed and unexposed areas through the decrease of hydrophobicity resulting from the loss of fluorine. Such contrast could be used for lithographic applications [8,9].

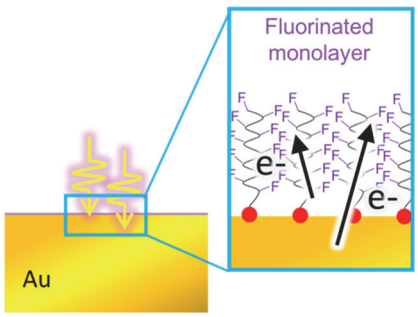

Fig. 1. Schematic of a monolayer of fluorinated carbon chains adsorbed on an Au substrate when it is irradiated with EUV photons. Photoelectrons generated upon the absorption of EUV photons (absorption mainly in the Au substrate) induce chemical change.

2. Experimental

Polycrystalline gold surfaces were prepared by sputter coating (Leica EM ACE600) silicon substrates with a layer of 50 nm of gold (adhesion layer: 5 nm of Chromium). The fluorinated thiol (3,4,5,6,7,8,9,10)-heptadecafluorodecanethiol (HFDT) was purchased from Sigma-Aldrich. The thiol was adsorbed on the Au surfaces by immersing the substrates in an ethanol solution of HFDT (3 mM, 24 h, RT).

Chemical changes induced by EUV photons were evaluated by means of Photoelectron Spectroscopy (PES) provided with a hemispherical analyzer with energy resolution ~ 100 meV at synchrotron IOM-CNR BEAR beamline station at Elettra in Trieste, Italy [10–12]. Monochromatized (aprox. 30 meV of resolution) photons of 92 eV were used as excitation energy.

The incoming light was linearly polarized (horizontally) orthogonal to the incidence plane (*s*-polarization ~ 97% of polarization degree) with light spot at sample ~ 400 × 140 μm^2 (horizontal × vertical). The angle of incidence was 45° with the electron analyzer positioned in normal emission. The impinging photons intensity at 92 eV was measured by an absolute (AXUV100) photodiode. Exposure doses were estimated according to beamline optics settings, light spot and impinging flux. To correct for possible beam fluctuation, the acquired data was accompanied with its relative photon flux, monitored on the last optical element (refocusing mirror) upstream of the sample.

To prevent exposure damage of the monolayer during the acquisition, the evolution of the photoelectron emission intensities was recorded starting on a fresh spot for each kinetic energy. This was achieved by using in-sequence acquisition, effectively correlating sample stage movement (xy) with kinetic energy tuning of the analyzer. In this way, stacks of data of photoelectron intensity versus dose at fixed kinetic energy were obtained. Finally, spectra were reconstructed from these stacks of data by extracting the values of intensity at identical dose for each kinetic energy.

Theoretical calculations on the HFDT molecule were performed with Gaussian 16 [13] using Density Functional Theory (DFT), and employing the B3LYP functional and 6-311G basis set.

3. Results and discussion

Photoelectron spectroscopy (PES), owing to its surface sensitivity was chosen to identify and quantify chemical changes induced by EUV photons on a self-assembled monolayer of fluorinated thiol adsorbed on polycrystalline gold, HFDT/Au. By using 92 eV as excitation energy, both the damage and the monitoring of the damage were conducted simultaneously, effectively reducing the possibility of undesired degradation commonly occurring when sample irradiation and PES measurement take place individually. The photoemission spectra recorded from the Au substrate and from HFDT/Au pristine sample (exposure of ca. 1 mJ/cm^2) are shown in Fig. 2. The zero of binding energy scale was set at the onset (Fermi level) of the bare Au valence spectrum.

In the spectrum of Au, two main broad non-symmetric peaks are observed from photoelectrons emitted by the 5 d orbitals ($5d_{5/2}$, 3 – 5 eV and $5d_{3/2}$, 5 – 8.5 eV) [14–17]. A broad feature arises from 14 eV on, that can either be attributed to the presence of nanometric aggregates on Au surface or to the detection of electrons generated during the photoelectron scattering through the Au. The spectrum of HFDT on Au clearly differs from the Au one. Two prominent peak envelopes in the 12.7 – 16.0 eV (A) and 8.0 – 12.7 eV (B) binding energy

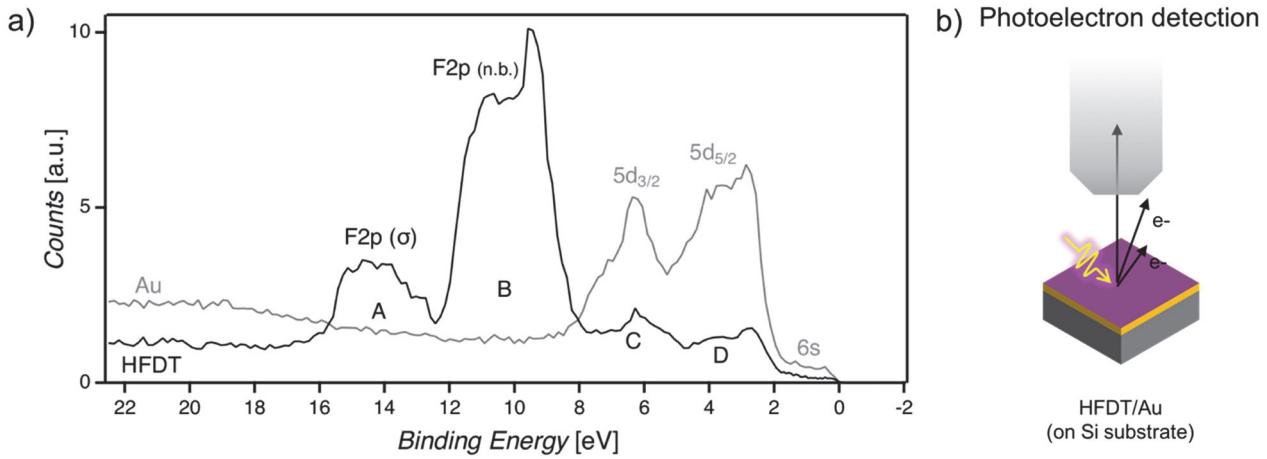

Fig. 2. a) Experimental photoelectron spectra recorded with 92 eV photon energy of the Au-coated substrate (grey) and of the HFDT/Au sample. b) Basic scheme of the PES experiment.

range are clearly distinguishable in the monolayer's spectrum. These exact features had been previously observed in photoelectron studies performed on analogous molecules with silane as anchoring group for silicon substrates [9]. In addition, the peaks arising from the Au 5d photoelectrons (C and D) are also visible, although with much lower intensity, reasonably ascribable to scattering attenuation through the film, as discussed below. It is expected that photoelectrons coming from the upmost levels of the valence band of the HFDT/Au system also contribute to the spectral lineshape in this region (see fittings below). No evident energy shifts are detected in the Au 5d peaks.

To assign the peaks in the PE spectrum of HFDT, the molecular orbitals (MO) of the molecule in the gas phase were calculated with density functional theory (B3LYP functional, 6-311G basis set). The representation of some selected MOs in the 25 eV to 0 eV binding energy range is shown in Fig. 3. The actual energy of the MOs can vary when the molecule is embedded in a monolayer adsorbed on Au, due to intermolecular interactions and to the bonding of the sulfur atom to the Au atoms at the substrate surface.

Yet, despite the energy shift in the theoretical calculations, it is reasonable to assign the broad peaks A and B to photoelectrons generated from the F 2p orbitals that are participating in different molecular orbitals, in line with previous assignments in the literature [9]. It is tempting to further distinguish between types of F 2p orbitals for these two regions. Photoelectrons contributing to peak B could be assigned to F 2p orbitals with a "non-bonding" character, as the calculated MOs in the range from 10 to 15 eV (represented by red lines in the energy diagram in Fig. 3) seem to be located on the F 2p orbital with a perpendicular orientation regarding the C-F bond.

DFT calculations also show that for MOs with lower energies (delimited by the purple lines in the energy diagram) the F 2p orbitals participate in what looks like σ bonds along the C-F bond. We presume that binding orbitals of this kind are the origin of the broad peak A at a higher binding energy range.

Although F s and p electrons have relatively high photon absorption cross-sections at 92 eV (~0.8 Mbarn/atom), and despite the high concentration of F atoms in the HFDT self-assembled monolayer (17 fluorine atoms per molecule), a high transmittance is estimated for this monolayer (~1.2 - 1.5 nm thickness, depending on the molecular packing). Using the atomic photon absorption cross-section as reported in the literature [18], the molar cross-section for the HFDT molecule is calculated to be 3.7×10^7 cm^2/mol. Assuming that there are approximately 3 - 4 molecules per square nm [19,20] ($5.0 - 6.6 \times 10^{-10}$ mol/cm^2), and taking into account the angle of incidence of the impinging photons, the estimated transmittance for such a layer would be in the range of 97-98%. Therefore, most of the light goes through the HFDT monolayer and is absorbed by the Au substrate (50 nm thickness, ~ 0% transmittance). However, the number of photoelectrons generated at the Au layer that reach the detector is much lower in the presence of the HFDT monolayer. We attribute this loss of intensity (~65%) of the Au 5d peaks to the scattering of the primary photoelectrons through the monolayer.

The evolution of the HFDT photoelectron spectrum with exposure at 92 eV is shown in Fig. 4. A clear bleach of the peaks assigned to the F 2p orbitals is observed, indicating that fluorine concentration in the monolayer decreases.

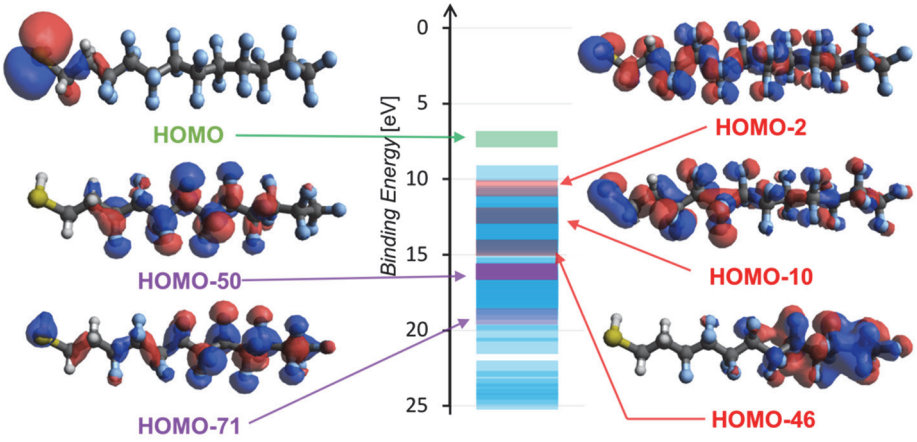

Fig. 3. Energy diagram of the HFDT molecular orbitals (MO) calculated with DFT in the gas phase (B3LYP, basis set 6-311G). Some selected MOs are represented.

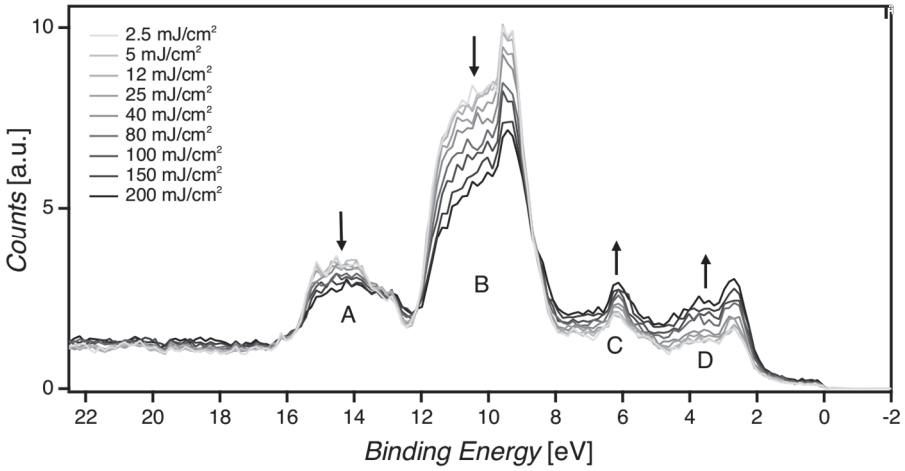

Fig. 4. Evolution of the photoelectron spectrum of HFDT/Au with EUV exposure (some selected doses are shown).

It has been previously reported that exposure of SAMs based on thiols featuring semi-fluorinated carbon-chains to low-energy electrons (10 eV) leads to the cleavage of C-F bonds and outgassing of fluorine, as well as C-C cleavage leading to the desorption of small fluorinated carbon chains [8]. Therefore, we assume that the fluorine loss induced by EUV exposure of the HFDT/Au system likely occurs via similar processes, as most of the chemical reactions that the monolayer undergoes are expected to be induced by the low-energy photoelectrons (typically ~< 80 eV) generated at the monolayer and the underlaying Au layer [21].

To estimate the rate of the EUV-induced changes, we calculated the relative areas (A/A0) of peaks A, B, C and D and plotted them as a function of dose in Fig. 5. The bleach of the peaks assigned to F 2p orbitals (A and B) reaches ~60% at 200 mJ/cm^2. Some molecular levels associated to sulfur and carbon atoms overlap with the Au valence peaks. Although the cross sections at 92 eV as well as the densities of sulfur and carbon atoms are lower than Au, these overlaps would explain the apparent different intensity ratio between $5d_{3/2}$ and $5d_{5/2}$ peaks in the pristine HFDT/Au sample compared to Au, as well as the slightly different increase rate of the two peaks upon EUV exposure [11].

In addition of the bleaching of peaks A and B, which we attribute to F loss, the spectra display changes at 13 eV and 17 eV (Fig. 4), which could be due to the creation of new electronic levels, i.e. new molecular orbitals. Partial loss of F-atoms is followed by the formation of highly reactive carbon-sites that can lead to the formation of mono-fluorinated carbon atoms and unsaturated C=C bonds and to cross-linking reactions between neighboring molecules. These examples have all been showed to take place under low-energy electron irradiation for similar systems [8].

And, as mentioned earlier, we expect similar

events to happen under EUV irradiation of the HFDT/Au system as a result of the interaction between the monolayer and the low-energy electrons (KE range from ~ 80 eV to 0 eV), mostly generated by the Au substrate [22,23]. These new molecular orbitals deriving from new bonds and chemical species can thus contribute to the modification of the spectral shape with increasing dose. However, the elucidation of the exact products that result from the 92 eV irradiation is out of the scope of this work.

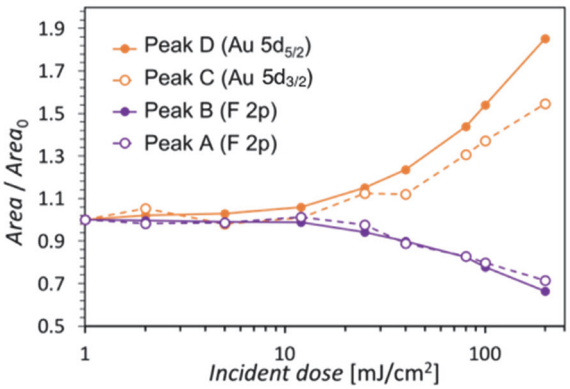

Fig. 5. Relative area of all peaks as a function of dose.

4. Conclusion

Photoelectron spectroscopy at a photon energy of 92 eV on monolayers of fluorinated thiols adsorbed on polycrystalline gold surfaces (HFDT/Au) revealed that EUV exposure of such a system leads to a remarkable loss of fluorine-containing species, reaching approximately 40% of fluorine content after a dose of 200 mJ/cm^2. We attribute the chemical processes that the monolayer undergoes upon EUV irradiation to the action of photoelectrons and secondary electrons generated both within the monolayer and the underlaying Au layer. While further work is needed to fully elucidate these phenomena, the extent of fluorine loss in the studied EUV dose range suggests that a considerable chemical contrast between exposed and unexposed areas is attained with this type of molecules, which could be used for lithography purposes.

Acknowledgements

Angelo Giglia (CNR-IOM) is acknowledged for dose evaluation and Konstantin Koshmak (CNR-IOM) for his valuable help during the experiment.

References

1. P. D. Ashby, D. L. Olynick, D. F. Ogletree, and P. P. Naulleau, *Adv. Mater.*, **27** (2015) 5813.
2. W. F. van Dorp, "Theory: Electron-Induced Chemistry", in "In Frontiers of Nanoscience – Materials and Processes for Next Generation Lithography", Elsevier, **11** (2016) p.115.
3. C. Zahlten, P. Gräupner, J. van Schoot, P. Kuerz, J. Stoeldraijer, and W. Kaiser, *Proc. SPIE*, **11177** (2019) 111770B.
4. A. Turchanin, M. Schnietz, M. El-Desawy, H. H. Solak, C. David, and A. Gölzhäuser, *Small*, **3** (2007) 2114.
5. E. Böhler, J. Warneke, and P. Swiderek, *Chem. Soc. Rev.*, **42** (2013) 9219.
6. J. Langer, M. Stano, S. Gohlke, V. Foltin, S. Matejcik, and E. Illenberger, *Chem. Phys. Lett.*, **419** (2006) 228.
7. S. G. Rosenberg, M. Barclay, and D. H. Fairbrother, *ACS Appl. Mater. Interfaces*, **6** (2014) 8590.
8. S. Frey, K. Heister, M. Zharnikov, and M. Grunze, *Phys. Chem. Chem. Phys.*, **2** (2000) 1979.
9. Y. Haruyama and S. Matsui, *Jpn. J. Appl. Phys.*, **54** (2015) 075202.
10. L. Pasquali, S. Mukherjee, F. Terzi, A. Giglia, N. Mahne, K. Koshmak, V. Esaulov, C. Toccafondi, M. Canepa, and S. Nannarone, *Phys. Rev. B - Condens. Matter Mater. Phys.*, **89** (2014) 1.
11. L. Pasquali, F. Terzi, R. Seeber, S. Nannarone, D. Datta, C. Dablemont, H. Hamoudi, M. Canepa, and V. A. Esaulov, *Langmuir*, **27** (2011) 4713.
12. http://www.elettra.trieste.it/elettra-beamlines/bear.html.
13. M. J. Frisch, G. W. Trucks, H. B. Schlegel, G. E. Scuseria, M. A. Robb, J. R. Cheeseman, G. Scalmani, V. Barone, G. A. Petersson, H. Nakatsuji, X. Li, M. Caricato, A. V. Marenich, J. Bloino, B. G. Janesko, R. Gomperts, B. Mennucci, and D. J. Hratch, Gaussian 16, Revision C.01. Wallingford CT p Gaussian, Inc., Wallingford CT (2016).
14. H. Piao and N. S. McIntyre, *J. Electron Spectros. Relat. Phenomena*, **119** (2001) 29.
15. A. Visikovskiy, H. Matsumoto, K. Mitsuhara, T. Nakada, T. Akita, and Y. Kido, *Phys. Rev. B - Condens. Matter Mater. Phys.*, **83** (2011) 1.
16. D. Wang, X. Cui, Q. Xiao, Y. Hu, Z. Wang, Y. M. Yiu, and T. K. Sham, *AIP Adv.*, **8** (2018) 6.
17. I. Lindau, P. Pianetta, K. Y. Yu, and W. E. Spicer, *Phys. Rev. B*, **13** (1976) 492.
18. B. L. Henke, E. M. Gullikson, and J. C. Davis,

At. Data Nucl. Data Tables, **54** (1993) 181.
19. S. W. Barton, A. Goudot, O. Bouloussa, F. Rondelez, B. Lin, F. Novak, A. Acero, and S. A. Rice, *J. Chem. Phys.*, **96** (1992) 1343.
20. H. Hinterwirth, S. Kappel, T. Waitz, T. Prohaska, W. Lindner, and M. Lämmerhofer, *ACS Nano*, **7** (2013) 1129.
21. R. M. Thorman, T. P. R. Kumar D. H. Fairbrother, and O. Ingolfsson, *Beilstein J. Nanotechnol.*, **6** (2015) 1904.
22. D. F. Ogletree, "Chapter 2 - Molecular Excitation and Relaxation of Extreme Ultraviolet Lithography Photoresists" in "Materials and Processes for Next Generation Lithography", A. Robinson and R. Lawson, Eds., Elsevier, **11** (2016) p.91.
23. J. Torok, R. Del Re, H. Herbol, S. Das, I. Bocharova, A. Paolucci, L. E. Ocola, C. Ventrice Jr., and E. Lifshin, *J. Photopolym. Sci. Technol.*, **26** (2013) 625.